Molecular Motion of Peroxy Radicals at Ends of Isolated and Nonisolated Polyethylene Chains Tethered on Powder Surface of Poly(tetrafluoroethylene) in a Vacuum

Masato Sakaguchi,*,† Katsuhiro Yamamoto,‡ Youhei Miwa,‡ Shigeo Hara,‡ Yusuke Sugino,‡ Shigeru Okamoto,‡ Masahiro Sakai,§ and Shigetaka Shimada‡

College of Nagoya Keizai University, 61, Uchikubo, Inuyama, 484-8503, Japan; Department of Materials Science & Engineering, Nagoya Institute of Technology, Gokiso-cho, Showa-ku, Nagoya 466-8555, Japan; and Research Center for Molecular-Scale Nanoscience, Institute for Molecular Science, 38, Nishigo-Naka, Myoudaiji, Okazaki 444-8585, Japan

Received April 26, 2004; Revised Manuscript Received August 4, 2004

ABSTRACT: Molecular motion of peroxy radicals at the ends of isolated (IPE) and nonisolated polyethylene (NIPE) chains tethered on the powder surface of poly(tetrafluoroethylene) (PTFE) was investigated in a vacuum in the temperature range from 3.4 to 223 K by electron spin resonance (ESR) and a spectral simulation. The IPE and the NIPE chains were produced by radical polymerization of ethylene initiated by PTFE radicals located on the surface. The isotropic and the anisotropic tumbling motions of the ends of IPE chains on the PTFE surface were observed, and their activation energies were estimated. At 223 K, the anisotropic tumbling motion mode of all the ends of IPE chains on the PTFE surface converted into a free rotational motion mode having a rate of 1.00×10^9 s^{-1}, in which the ends were protruding from the PTFE surface. The ends of IPE chains had noninteractions with both neighboring intra- and interchains of IPE. In contrast, the isotropic and the anisotropic tumbling motions of the ends of NIPE chains on the PTFE surface were slower than those of IPE chains. Even at 223 K, the tumbling motion of the ends on the surface still had anisotropic rates of 1.18×10^8 and 6.25×10^8 s^{-1}. The slow and anisotropic rates of the ends of NIPE chains on the PTFE surface were due to the interactions with both neighboring intra- and interchains of NIPE.

Introduction

Many studies have been reported for molecular motions of polymer chains in the bulk. They showed that a molecular motion of polymer chains is strongly affected by a surrounding matrix. Below a glass transition temperature (T_g), for example, a molecular motion of polymer main chains is highly limited due to the rigidity resulting from a huge degree of cooperativeness with surrounding interpolymer chains.[1,2] Mattice et al.[3−5] investigated the chain mobility of the surface and the interior of very thin films composed of amorphous PE using a Monte Carlo simulation on the basis of the rotational isomeric state model and reported that the chains on the surface are more mobile than in the interior and the chain ends are predominant at the surface. Kajiyama et al.[6−8] observed the reduction of T_g at polystyrene film surface by scanning force microscopy and lateral force microscopy measurements. The reduction in T_g was attributed to the excess free volume generated by the chain ends at the surface. If an isolated single polymer chain was obtained, the mobility of the polymer chain with noncooperative motion, i.e., without interaction of surrounding interpolymer chains, could be high even below T_g. An isolated polymer chain could be obtained in a gaseous condition. But it is impossible because it decomposes during gasification process. From another viewpoint, an isolated polymer chain could be defined as a chain having huge space around the chain. If the end of polymer chain has a large space, a molecular mobility of the end must be very high due to noninteraction with interpolymer chains. In previous papers,[9−15] we have reported that the isolated polymer chains tethered on the surface of PTFE in a vacuum were produced, and the ends of isolated polymer chains had high mobility even below their T_g's. For example, the ends of isolated polyethylene (PE) chains tethered on the surface of PTFE in a vacuum had two sites exchange motion between two β protons of a chain end-type free radical even at 2.6 K,[12] which is far below T_g (148 K)[16] of PE in the bulk. At 77 K, the motion of the ends showed a free rotational mode due to the ends protruding from the PTFE surface.[9−11] Unfortunately, the activation energy (E_a) of a transition from the slow tumbling motion to the free rotational motion could not be estimated by a restriction of the simulation program. On the other hand, the temperature-dependent ESR spectra of the peroxy radicals at the ends of isolated polymer chains tethered on the surface of PTFE showed that the mobile fraction of the ends increased with increasing temperature.[17−19] The mobile fraction reached to 50% around 120 K, and ΔH and ΔS were estimated by a simulation program.[19] However, we could not obtain both a mode and a rate of the motion of peroxy radicals due to a restriction of the program.

This paper focuses on the rates, the modes, and activation energies of the motions of peroxy radicals at the ends of IPE and NIPE chains tethered on the surface of PTFE in a vacuum, which were fitted by using a modified simulation program.

Experimental Section

Materials and ESR Measurement. PTFE powder (Aflon G80, Asahi Glass Co., Ltd.) was used without further purification. Ethylene (Takachiho Co., ltd) was purified by the freeze−pump−thaw method.

† College of Nagoya Keizai University.
‡ Nagoya Institute of Technology.
§ Institute for Molecular Science.
* Corresponding author: phone +81-572-21-3420, Fax +81-572-21-3420, e-mail sakaguch@nagoya-ku.ac.jp.

10.1021/ma049194j CCC: $27.50
Published on Web 09/24/2004

The PE chains tethered on the powder surface of PTFE in a vacuum were produced as follows: The PTFE powder (1.6 g) in a glass-ball-mill was evacuated at 10^{-4} Torr at 333 K for 4 h, and ethylene monomer (1.44×10^{-5} or 6.06×10^{-4} mol) was introduced to the glass-ball-mill. The glass-ball-mill was sealed off, set in Dewar vessel filled with liquid nitrogen, and milled by a homemade vibration-ball-mill apparatus.[20] PTFE powder was mechanically fractured with ethylene monomer for 21 h at 77 K in a vacuum. After milling, the whole glass-ball-mill with ESR sample tube attached to the top of the mill was placed in liquid nitrogen, and the powdered sample was dropped into the ESR sample tube within 1 s by turning the glass-ball-mill upside down. After the ESR observation of propagating radicals, alkyl radicals at the ends of polyethylene ($-CH_2-CH_2^{\bullet}$), oxygen gas at 215 Torr was introduced into the glass-ball-mill at 77 K, and the conversion reaction from the propagating radicals to the peroxy radicals ($-CH_2-CH_2-OO^{\bullet}$) was promoted by a successive annealing. After a complete oxidation of the propagating radicals, residue oxygen was eliminated.

ESR spectra were observed at a microwave power level of 0.1 mW to avoid power saturation and with 100 kHz field modulation using a Bruker ESP 300E spectrometer (X-band) equipped with a helium cryostat (Oxford ESR 900) and a temperature controller (OXFORD ITC4).

Spectral Simulation. Binsch et al.[21,22] had reported a method to calculate a line shape equation of exchange-broadened NMR spectra in solution resulting from density matrix theory in the Liouville representation. This equation is, as expected, identical with that derived from the modified Bloch equations. Heinzer[23] has employed Binsch's method to calculate a line shape equation of exchange-broadened ESR spectra in solution, in which g and hyperfine splitting tensors were isotropic. Heinzer's method was successfully employed to exhibit a line shape of exchange-broadened ESR spectra in solution.[23]

We have modified Heinzer's method[23] to calculate a line shape equation of exchange-broadened ESR spectra in the solid state, in which g and hyperfine splittings have anisotropic tensors. As has been shown,[23] the complex magnetization, Z, is given by

$$Z = -iC\mathbf{S}^{-}\sum_{j=1}^{n_L} D_j \mathbf{M}_{0j}{}^{-1}\mathbf{P} \tag{1}$$

According to Heinzer's definition,[23] $\mathbf{M_0}$ is a complex non-hermitian matrix of dimension $N = n_C n_L$, with n_C = number of chemical configurations and n_L = number of lines. $\mathbf{P}$ is a population. $\mathbf{S}^{-}$ is shift operator. The degeneracy of a transition is denoted by D_j. The C denotes a scaling factor. The imaginary part of Z yields the absorption line shape equation directly. $\mathbf{M}_{0j}$ can be decomposed into a constant matrix, $\mathbf{F}$, and a scalar matrix, $iH\mathbf{E}$:

$$\mathbf{M}_{0j} = \mathbf{F}_j + iH\mathbf{E}$$

with

$$\mathbf{F}_j = \sum_{r=1}^{n_c}\sum_{s=1}^{n_c}[-i\delta_{rs}(H^{\circ}{}_r + \sum_{\alpha=1}^{n_A} A_{r\alpha}) - \delta_{rs}(1/T_2) - \delta_{rs}\sum_{n\neq r}^{n_c} K_m + (1-\delta_{rs})K_{sr}]$$

$$K_{sr} = (1/\tau_r)(h/2\pi)\omega_{0,r}/(g_r\beta)$$

$$1/T_2 = (1/T_{2,r})(h/2\pi)\omega_r/(g_r\beta)$$

$$H^{\circ}{}_r = (h/2\pi)\omega_r/(g_r\beta)$$

$$g^2{}_r = g^2{}_{r1}\cos^2\phi\sin^2\theta + g^2{}_{r2}\sin^2\phi\sin^2\theta + g^2{}_{r3}\cos^2\theta$$

$$A^2{}_r = A^2{}_{r1}\cos^2\phi\sin^2\theta + A^2{}_{r2}\sin^2\phi\sin^2\theta + A^2{}_{r3}\cos^2\theta$$

The values K_{sr} are treated as rate constants for transfer from r to s. The value τ_r is a lifetime for the r conformation. $H^{\circ}{}_r$ is an electronic Zeeman interaction of r conformation. $1/T_2$ is a line width. The g_r and A_r are g values and hyperfine splittings at r conformation. The last two terms, $-\delta_{rs}\sum_{n\neq r}^{nc} K_m + (1-\delta_{rs})K_{sr}$, are responsible for the intramolecular exchange. In our simulation, K_{sr} and a conformation were adopted into f_r and a site. All values are exhibited with a magnetic field unit instead of a frequency unit.

We assume that $\mathbf{M}_{0j}$ in our practical application can always be reduced to a diagonal matrix by the transformation[21-23]

$$\mathbf{U}_j{}^{-1}\mathbf{M}_{0j}\mathbf{U}_j = \mathbf{U}_j{}^{-1}(\mathbf{F}_j + iH\mathbf{E})\mathbf{U}_j \tag{2}$$

Since $\mathbf{F}_j$ and $\mathbf{E}$ commute, the same transformation also diagonalizes $\mathbf{F}_j$. Hence

$$\mathbf{M}_{0j}{}^{-1} = \mathbf{U}_j(\Lambda_j + iH\mathbf{E})^{-1}\mathbf{U}_j{}^{-1} \tag{3}$$

Λ_j represents eigenvalues of $\mathbf{F}_j$.

Substitution of eq 3 in eq 1 and rewriting by the elements yield

$$Z = -iC\sum_{j=1}^{n_L}\sum_{\mu=1}^{n_C} D_j \sum_{\lambda=1}^{n_C} S_\lambda{}^{-} U_{j\lambda\mu}\sum_{l=1}^{n_C} U_{j\mu l}{}^{-1} P_l (\Lambda_{j\mu} + iH)^{-1}$$

Defining ashape vector, $\mathbf{S}_j$, by the elements

$$S_{j\mu} = D_j \sum_{\lambda=1}^{n_C} S_\lambda{}^{-} U_{j\lambda\mu}\sum_{l=1}^{n_C} U_{j\mu l}{}^{-1} P_l$$

we get

$$Z = -iC\sum_{j=1}^{n_L}\sum_{\mu=1}^{n_C} S_{j\mu}(\Lambda_{j\mu} + iH)^{-1}$$

The absorption, Y, is propotional to the imaginary part of Z.

$$dY/dH = -C\ \mathrm{Imag}[\sum_{j=1}^{n_L}\sum_{\mu=1}^{n_C} S_{j\mu}(\Lambda_{j\mu} + iH)^{-2}] \tag{4}$$

The imaginary part of $\Lambda_{j\mu}$ defines the position. The real parts of $S_{j\mu}$ and $(2/\sqrt{3})\Lambda_{j\mu}$ define relative intensity and the line width of a line $j\mu$.

On the computation of the ESR spectra, we assumed that each radical was trapped in three sites for each residence time (τ_1, τ_2, τ_3) and tumbled into each site at a rate $f = \tau^{-1}$. Each population of the sites was assumed to be equal. Three sites were defined as follows: site 1 (g_1, g_2, g_3), site 2 (g_2, g_3, g_1), and site 3 (g_3, g_1, g_2), which were composed of the same principal values of g-tensor.

Results and Discussion

Production of Chain End Alkyl Radicals Tethered on the Powder Surface of PTFE. We have reported[9-15,17-19,24-26] that the vibration-ball milling of PTFE powder in a vacuum at 77 K produced the PTFE mechano radicals, chain-end-type fluoroalkyl radicals, $-CF_2-CF_2^{\bullet}$, which were trapped on the fresh surface of PTFE, and the PTFE mechano radicals initiated radical polymerizations of several monomers. The PTFE fractured with ethylene monomer at 77 K in a vacuum produced the PE chains having propagating radicals at the ends and tethering on the fresh powder surface of PTFE. The five-line ESR spectrum of the milled PTFE with ethylene monomer (1.44×10^{-5} mol) was observed at 77 K (shown in Figure 1 with the solid line and five open circles). The five-line spectrum indicates that PTFE mechano radicals initiated a block copolymerization of ethylene monomer in a vacuum at 77 K.[9-11]

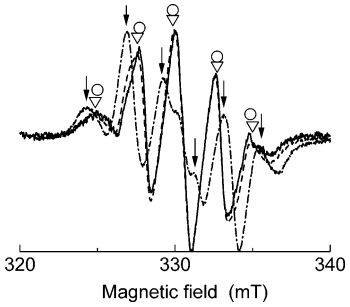

Figure 1. ESR spectra of the propagating alkyl radicals of PE at the ends of IPE and NIPE chains tethered on the powder surface of PTFE: solid line and open circles, spectrum of the as-fractured PTFE with ethylene monomer 1.44×10^{-5} mol; broken line and open triangles, spectrum of the as-fractured PTFE with ethylene monomer 6.06×10^{-4} mol; dot−dashed line and arrows, spectrum annealed at 143 K.

The wing peaks[24] arising from the PTFE mechano radicals were not observed. Thus, the conversion reaction from PTFE mechano radicals to propagating alkyl radicals of PE was carried out completely during the milling. To consume the residue of ethylene monomer, the sample was annealed at 125 K for 60 min; that temperature is above melting temperature of ethylene, 104 K.[27] The annealing did not make a change in the ESR spectrum. Assuming no residue of the monomer, the average polymerization degree (*PD*) of PE was estimated at 80 by the concentrations of ethylene monomer and PTFE mechano radicals (6.8×10^{16} radicals/g) located on the surface.[10] The radius of gyration ($R_g = (C_\infty(2PD - 1)a_b^2/6)^{1/2}$) of PE was estimated as 2.1 nm on the basis of the *PD* of PE, carbon−carbon bond length ($a_b = 0.15351$ nm)[28] and characteristic ratio ($C_\infty = 6.7$)[29] of PE in 1-dodecanol solution at 411 K. On the other hand, Mattice et al. have reported that the R_g values were 1.1,[5] 1.3 ± 0.1,[3] and 1.5 nm[4] on the Monte Carlo simulation for chain mobility of very thin films ($\sim 2R_g$ to $\sim 8R_g$) composed of amorphous PE: $C_{60}H_{122}$, $C_{100}H_{202}$, and $C_{120}H_{242}$, respectively. In addition, the parallel component ($R_{g,xy} = ((R_{g,x}^2 + R_{g,y}^2)/2)^{1/2})$) and the perpendicular component ($R_{g,z}$) of the radius of gyration of $C_{80}H_{162}$ on the surface are 1.1 and 0.6 nm.[5] The $R_{g,xy}$ and $R_{g,z}$ of $C_{120}H_{242}$ are 1.8 and 0.4 nm.[4] Furthermore, Mattice et al.[5] have introduced the relative shape anisotropy (k^2), which is defined through asphericity and acylindricity. The k^2 values should be 0 if the object is a perfect sphere and 1 if it is a perfect rod. The k^2 values have been reported as 0.43−0.47 in the simulation. Thus, the shape should be intermediate between a perfect sphere and a perfect rod. On the other hand, Mattice et al.[30] have reported that the relationship between the characteristic ratio of a finite chain (C_n) and C_∞ is given by

$$C_n/C_\infty = 1 + (1/n)C_\infty^{-1}[\mathrm{d}C_n/\mathrm{d}(1/n)]_{1/n=0} \qquad (5)$$

where n is the number of bonds, $C_\infty = 6.81$, and C_∞^{-1}-$[\mathrm{d}C_n/\mathrm{d}(1/n)]_{1/n=0} = -5.2$ for PE. If eq 5 is employed to calculate C_n, the R_g is given by

$$R_g = (C_n n a_b^2/6)^{1/2} \qquad (6)$$

When eqs 5 and 6 are employed to $C_{60}H_{122}$, $C_{100}H_{202}$, and $C_{120}H_{242}$, the values of R_g are calculated as 1.2, 1.6, and 1.8 nm. Thus, we employed eqs 5 and 6 to calculate the R_g value. In our experiment, in which $n = 159$ ($= 2PD - 1$) and $C_n = 6.59$, the R_g was calculated to be 2.0 nm for the 80 of *PD*. The shape should be intermediate between a perfect sphere and a perfect rod on the basis of the results of Mattice's simulation.

On the other hand, the area per tethered point on the PTFE surface was calculated to be at 31 nm^2 on the basis of the concentration of PTFE mechano radicals located on the surface and specific surface area (2.1 m^2/g).[10] Assuming the area of a circle for the 31 nm^2, its radius (R_t) per tethered point is to be 3.1 nm. If R_L ($= R_g/R_t$) < 1.0, a tethered PE chain cannot contact and entangle with neighboring PE chains. The R_L of PE having 80 *PD* was estimated to be 0.65. Thus, the contacts and the entanglements with neighboring PE chains cannot take place. In addition, each chain does not aggregate because the chain is tethered on the PTFE surface by a covalent bond. Furthermore, PE is immiscible with PTFE. Thus, the PE chain has free motion, noncooperative with interpolymer chain tethered on the PTFE surface, and has a large space around the chain. We called the PE chains tethered on the powder surface of PTFE in a vacuum as "isolated PE (IPE) chains".

The long PE chains, which also have propagating radicals at the ends, tethered on the powder surface of PTFE in a vacuum were produced by the same procedure as in the case of IPE chains except high concentration (6.06×10^{-4} mol) of ethylene monomer. The five-line ESR spectrum of the as-milled sample was observed at 77 K (shown in Figure 1 with the broken line and five open triangles). The five-line spectrum seems nearly identical with that of IPE chains. The five-line spectrum indicates that PTFE mechano radicals also initiated block copolymerization of ethylene monomer in a vacuum at 77 K and were completely converted to propagating alkyl radicals of PE because no wing peak was observed. To consume the residue of the ethylene monomer, the sample was successively annealed at 125 K for 57 min and at 143 K for 15 min. After the successive annealing, the five-line spectrum changed to a two-component spectrum consisting of five- and six-line signals (shown in Figure 1 with the dot−dashed lines and six arrows). The six-line spectrum strongly suggests that the propagating radicals attached to the ends of long PE chains, and the molecular motion of the propagation radicals was restricted by inter-PE chains.[9,10] Assuming complete consumption of the ethylene monomers, the average *PD* of PE was estimated 3.35×10^3 by a similar procedure as for IPE chains. The R_g of PE chain was estimated to be 13.4 nm on the basis of $n = 6699$ and $C_n = 6.80$. The R_L was calculated 4.32. Thus, the PE chains tethered on the powder surface of the PTFE interact with neighboring inter-PE chains, probably have entanglements with neighboring inter-PE chains, and result in a cooperative motion with interpolymer chains. The molecular motion should be restricted by interpolymer chains. We called the long PE chains tethered on the powder surface of PTFE in a vacuum as "nonisolated PE (NIPE) chains".

Oxidation of Propagating Radicals at the End of PE Chains Tethered on the Powder Surface of PTFE. The as-fractured sample of IPE chains shows a five-line ESR spectrum at 77 K due to the propagating radicals of PE (Figure 2a). The sample was contacted with oxygen at 77 K and was kept at 77 K for 40 min (Figure 2b). Then, the sample was successively annealed at 143 K for 15 min (Figure 2c) and 45 min (Figure 2d).

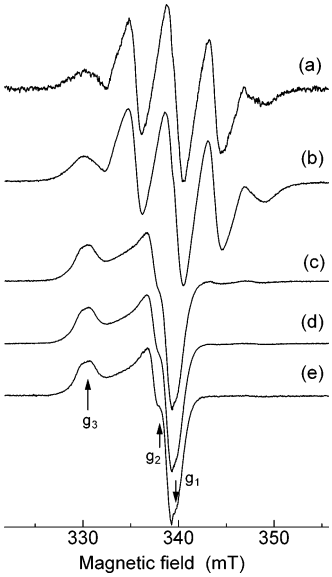

Figure 2. Spectral change with advancing the oxidation reaction from the chain end-type alkyl radicals at the ends of IPE chains to the peroxy radicals: (a) as-fractured PTFE with ethylene monomer at 77 K; (b) after contact with oxygen molecules at 77 K; (c) after annealed at 143 K for 15 min; (d) after successive annealing at 143 K for 45 min; (e) after successive annealing at 156 K for 30 min. All ESR spectra were observed at 77 K. The arrows show three g values: $g_1 = 2.0029$, $g_2 = 2.0079$, and $g_3 = 2.0372$.

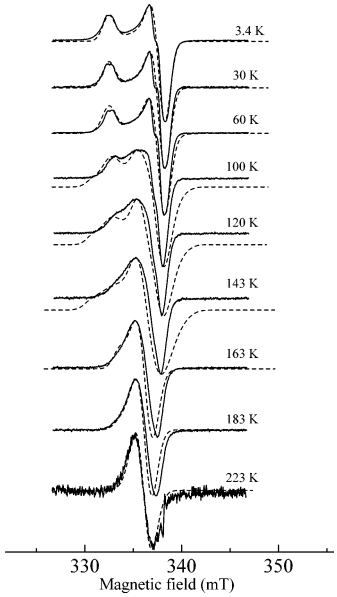

Figure 3. Temperature-dependent ESR spectra of peroxy radicals at the ends of IPE chains: solid lines, observation spectra; broken lines, simulation spectra using the three g values $g_1 = 2.0029$, $g_2 = 2.0079$, and $g_3 = 2.0372$. See text for simulation details.

The ESR spectrum shows a characteristic powder pattern of peroxy radicals.[17−19,31] To make complete conversion of the propagating radicals into the peroxy radicals, the sample was annealed at 156 K for 30 min (Figure 2e). After the successive annealing, the residue oxygen was eliminated by an evacuation. Then, the peroxy radicals at the ends of IPE chains tethered on the surface of PTFE in a vacuum were obtained. In the case of NIPE chains, the peroxy radicals were obtained by the same procedure as in the IPE chains.

Molecular Motions of Peroxy Radicals at the Ends of IPE and NIPE Chains. The ESR spectra of peroxy radicals at the ends of IPE chains tethered on the powder surface in a vacuum were observed in the temperature range from 3.4 to 223 K, shown in Figure 3 with the solid lines. The simulation spectra are shown with the broken lines. The simulated spectrum at 3.4 K using the three principal values of g-tensor ($g_1 = 2.0029$, $g_2 = 2.0073$, $g_3 = 2.0372$) in a rigid-limit model is in good agreement with the observed spectrum. The spectrum observed at 3.4 K indicates that the molecular motion of peroxy radicals is in a rigid-limit state. The shape of the observed spectrum at 30 K looks like similar to that of the observed at 3.4 K, but the depth of the valley between the signal positions of g_2 and g_3 is slightly different. The difference suggests that some kind of motion occurs at the temperature. The observed spectrum at 30 K is in good agreement with the simulated spectrum, which was calculated by the using the three g values of the rigid limit model and an isotropic rate ($f_1 = f_2 = f_3$) of 2.00×10^6 s^{-1}. This result indicates that the onset temperature of the isotropic tumbling motion of the peroxy radicals was 30 K. Each observation spectrum changed its shape with increasing temperature.

Figure 4A shows the temperature dependence of f, which is obtained by the spectral simulation on the basis of the same principal g values. The three values of f_1, f_2 (open circles), and f_3 (closed circle) are equivalent, i.e., f is isotropic, and increases with an increase in temperature below 113 K. The isotropy of f was broken at 120 K. The anisotropic f, which indicates an anisotropic tumbling motion, increased with increasing temperature. The anisotropic f at 163 K, for example, was obtained at 5.26×10^8 s^{-1} ($f_1 = f_2$) and 1.25×10^8 s^{-1} (f_3). The average rates ($f_{av} = (f_1 + f_2 + f_3)/3$) are shown in Figure 4A with triangles. The f_{av} increased with increasing temperature (Figure 4A), but the anisotropy of the spectrum decreased with increasing temperature (Figure 3). Finally, the observed spectrum at 223 K shows a symmetric singlet spectrum (Figure 3). The simulated spectrum at 223 K is in good agreement with the observation spectrum using the isotropic and high f of 1.00×10^9 s^{-1}.

Padding and Briels[32] carried out a molecular dynamics simulation of $C_{120}H_{242}$ in melts, which is on the basis of "an entanglement", which should dynamically slide along the backbone of the chain, and an entanglement should disentangle if demanded by the topology of the chain. Only a few of these dynamical entanglements are expected to be entanglements in the ordinary definition. For instance, the $C_{120}H_{242}$ chain is generally considered not to be entangled, yet many "entanglements" occur in the simulation. Actually, the entanglement length corresponds to a length of C_{40} in the chain.[32]

In the case of IPE chains, we consider that only a few "weak and dynamic pseudo-entanglement", which should disentangle and disappear at elevated temperature, are expected to be entanglements.

The temperature-dependent ESR spectra can be explained by three kinds of motional modes as follows: (i) An isotropic tumbling motion of the ends on the PTFE surface having isotropic and slow rate: The IPE chain in a very low-temperature region formed one or several "weak and dynamic pseudo-entanglements", which were composed of a single IPE chain tethered on the surface of PTFE in a vacuum. The isotropic tumbling motion below 113 K did not depend on the weak and dynamic pseudo-entanglements because the isotropic tumbling

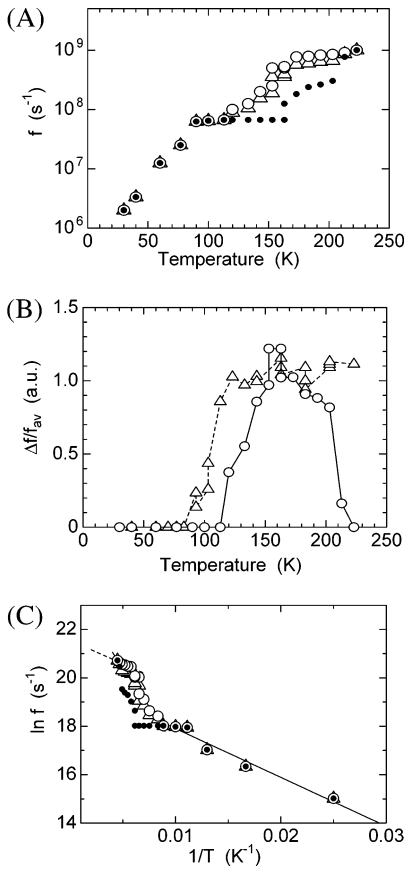

Figure 4. (A) Temperature dependency of the rates $f = \tau^{-1}$ of the tumbling motion of the peroxy radicals at the ends of IPE chains tethered on the powder surface of PTFE in a vacuum, where τ is a residence time at the site. IPE chains: open circles, $f_1 = f_2$; closed circles, f_3; open triangles, average f ($f_{av} = (f_1 + f_2 + f_3)/3$). (B) Temperature dependency of $\Delta f/f_{av}$. IPE chains, open circles; NIPE chains, open triangles. The solid and the broken lines are to guides for the eye. (C) Arrhenius plot of tumbling motion of the ends of the IPE chains. Open circles, $f_1 = f_2$; closed circles, f_3; open triangles, f_{av}. The two solid lines were the lines fitted to the data by least squares on the basis of the f_{av}.

motion needs a small-scale space. (ii) An anisotropic tumbling motion of the ends on the PTFE surface having anisotropic rates: The tumbling motion came vigorous with increasing temperature in the range 120−160 K; the tumbling motion requires larger space for the motion. Then, the motion of the ends of the IPE chains was restricted by the weak and dynamic pseudo-entanglements and resulted in an anisotropic tumbling motion with anisotropic rates. Above 160 K, the weak and dynamic pseudo-entanglements came loose. (iii) A free-rotational mode of the ends protruding from the PTFE surface having high and isotropic rate: The weak and dynamic pseudo-entanglements disentangled and disappeared at 223 K. The ends of IPE chains protruding far from the surface were free from the intra- and interchains of IPE and were in a free rotational mode with the isotropic and high rate.

Figure 4B shows a temperature dependence of a degree of anisotropy of the rate defined as $\Delta f/f_{av}$, where Δf is ($f_1 - f_3$). The $\Delta f/f_{av}$ values of the IPE chains are shown with open circles. The solid line through the data is to guide the eye. The isotropic tumbling motion was dominant below 113 K, while the nonzero $\Delta f/f_{av}$ value appeared at 120 K; i.e., the anisotropic tumbling motion restricted by the weak and dynamic pseudo-entanglement came dominant instead. The increase of $\Delta f/f_{av}$ with increasing temperature below 160 K suggests that the anisotropic tumbling motion came more vigorous with increasing temperature and was more restricted by the weak and dynamic pseudo-entanglements. The $\Delta f/f_{av}$ reached maximum around 160 K. Above 160 K, the $\Delta f/f_{av}$ decreased with increasing temperature, and finally, the $\Delta f/f_{av}$ came back to zero. This result can be explained that the weak and dynamic pseudo-entanglements come loose with increasing temperature, the degree of the restriction to the motion becomes negligible, and finally, the weak and dynamic pseudo-entanglements melt and disappear at 223 K. The ends of IPE protrude from the surface and freely rotate with zero value of $\Delta f/f_{av}$, i.e., at isotropic and high rate.

Figure 4C shows the Arrhenius plots of ln f vs $1/T$. The open circles, the closed circles, and the open triangles exhibit $f_1 = f_2$, f_3, and f_{av}, respectively. The first activation energy (E_{a1}) of the isotropic tumbling motion in the temperature range from 30 to 113 K was calculated to be at 1.68 kJ/mol. The solid line was the one fitted to the data by least squares. Since the tumbling motion with isotropic f of the ends of IPE chains on the PTFE surface in a vacuum has very small value of E_{a1}, the tumbling motion is probably something like "a tunneling motion" on the PTFE surface in a vacuum. The second activation energy (E_{a2}) due to the anisotropic tumbling motion in the temperature range from 120 to 213 K was estimated at 5.45 kJ/mol by the Arrhenius plot on the basis of the values of f_{av}, in which the solid line was the one fitted to the data by least squares. The E_{a2} value is about 3 times larger than E_{a1}. The anisotropic tumbling motion probably is a large-scale motion on the PTFE surface compared to the isotropic tumbling motion. The broken line is the one fitted to the data by least squares on the basis of the values of f_1 and passes through the isotropic f of 1.00×10^9 s^{-1} at 223 K. The third activation energy (E_{a3}) over 223 K may be speculated to be 1.60 kJ/mol. The very low E_{a3} also suggests that the motional mode of the ends of IPE chains at 223 K is quite different from the anisotropic tumbling motional mode below 213 K. The ends of IPE chains protrude from the surface and freely rotate in the space far from the surface.

On the contrary, the temperature-dependent ESR spectra of peroxy radicals at the ends of NIPE chains tethered on the powder surface of PTFE in a vacuum in the temperature range from 3.4 to 223 K are shown in Figure 5 with the solid lines. The simulation spectra are shown with the broken lines. The simulated spectrum at 3.4 K using the three principal values of g-tensor ($g_1 = 2.0019$, $g_2 = 2.0079$, $g_3 = 2.0368$, and $g_{iso} = 2.0155$) in a rigid-limit model is in good agreement with the observed spectrum. This result indicates that the molecular motion of peroxy radicals was in a rigid-limit state. The g values used the simulation are slightly different from the g values ($g_1 = 2.0029$, $g_2 = 2.0079$, $g_3 = 2.0372$, and $g_{iso} = 2.0157$) in a rigid limit spectrum of the ends of IPE chains. The slightly difference of g values may be due to a difference of a matrix around the ends of NIPE chains on the PTFE surface. The shape of the observed spectrum at 40 K looks like similar to that of the observed at 3.4 K, but the depth of the valley between the signal positions of g_2 and g_3 is slightly different. The difference suggests that some kind of motion occurs at the temperature. The observed spectrum at 40 K is in good agreement with the

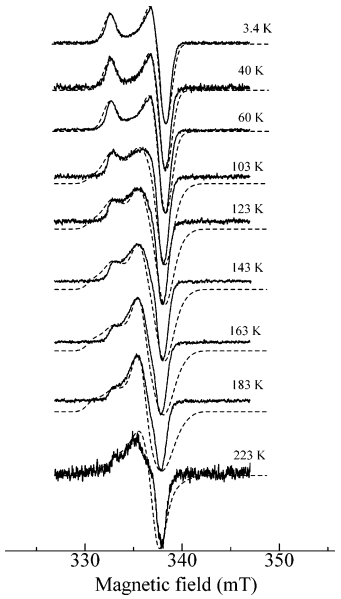

Figure 5. Temperature-dependent ESR spectra of the peroxy radicals at the ends of NIPE chains tethered on the powder surface of PTFE in a vacuum: solid lines, observation spectra; broken lines, simulation spectra using the three g values $g_1 = 2.0019$, $g_2 = 2.0079$, and $g_3 = 2.0368$. See text for simulation details.

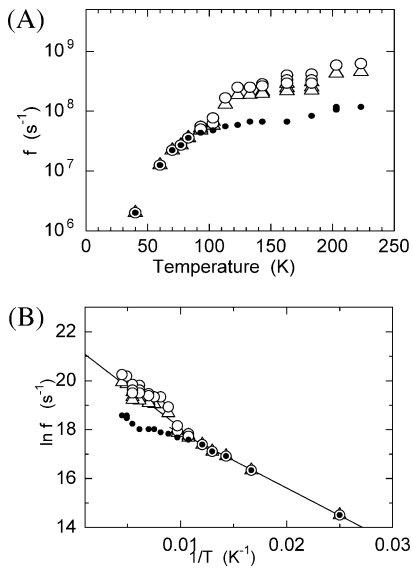

Figure 6. (A) Temperature dependency of the rates of the tumbling motion of the peroxy radicals at the ends of NIPE chains tethered on the powder surface of PTFE in a vacuum. (B) Arrhenius plot of tumbling motion of the ends of the NIPE chains. The solid line was the one fitted to the data by least squares on the basis of the f_{av}. The definition of symbols is the same as that in Figure 4.

simulated spectrum using the same principal values and an isotropic f of 2.00×10^6 s^{-1}. The onset temperature of the isotropic tumbling motion on the PTFE surface with isotropic f was 40 K. The higher onset temperature than that of IPE chains is probably attributed to real entanglements among inter-NIPE chains and high chain density arising from large R_L (= 4.32). The ESR spectra changed their shapes with increasing temperature. The temperature dependence of f is shown in Figure 6A with open circles (f_1 and f_2) and closed circles (f_3). The open triangles exhibit f_{av}. Figure 6A shows that the values of f_1, f_2, and f_3 are identical with each other below 83 K. The isotropic rate assigned to the isotropic tumbling motion increased with an increase in temperature below 83 K. However, the isotropy of f was broken at 93 K. The values of the anisotropic f increased with increasing temperature. The anisotropic rates, for example, at 163 K were estimated at 2.94×10^8 s^{-1} ($f_1 = f_2$) and 6.67×10^7 s^{-1} (f_3). The rates are slower than those of IPE chains. The ESR spectrum observed at 223 K still showed an anisotropic shape (Figure 5, the solid line), and the simulation spectrum (the broken line) was obtained using the anisotropic rates of 6.25×10^8 s^{-1} ($f_1 = f_2$) and 1.18×10^8 s^{-1} (f_3). The anisotropic rate indicates that the ends of NIPE chains on the PTFE surface are not in free rotational mode but in the anisotropic tumbling motional mode on the surface.

The values of $\Delta f/f_{av}$ are shown in Figure 4B with open triangles. The broken line through the data is to guide the eye. The onset temperature of nonzero value of $\Delta f/f_{av}$ was 93 K. The lower onset temperature of the anisotropic tumbling motion of NIPE chains compared to that of IPE chains is probably attributed to the real and high density of entanglements among inter-NIPE chains. The anisotropic tumbling motion became more activated with increasing temperature and more restricted by the entanglements and inter-NIPE chains. The $\Delta f/f_{av}$ value increased with increasing temperature and reached a maximum around 160 K. However, the value of $\Delta f/f_{av}$ did not decrease in the temperature range from 160 to 223 K, and even at 223 K $\Delta f/f_{av}$ was not zero but still a large value. The results indicate that the ends of NIPE chains were still in the anisotropic tumbling motional mode on the surface of PTFE because the real entanglements among inter-NIPE chains do not melt.

Figure 6B shows the Arrhenius plots of the tumbling motion, in which the open circles, the closed circles, and the open triangles exhibit $f_1 = f_2$, f_3, and f_{av}, respectively. The E_{a1} in the temperature range from 40 to 83 K was calculated to be at 1.87 kJ/mol using the isotropic f. The solid line was the one fitted to the data by least squares. The anisotropic tumbling motion on the PTFE surface with anisotropic f was observed in the temperature range from 93 to 223 K. The E_{a2} of the anisotropic tumbling motion was calculated to be 2.77 kJ/mol on the basis of the f_{av}. The value of E_{a2} is nearly identical with that of E_{a1}. Thus, the isotropic and the anisotropic tumbling motional modes on the PTFE surface are probably equal to each other. Even at 223 K, the ends of NIPE chains were probably located on the PTFE surface, which was deduced from the motion of the ends having large anisotropic rate. Thus, the motion of the ends on the PTFE surface was restricted by the intra- and the interchains of NIPE.

Conclusion

The IPE and the NIPE chains were produced by radical polymerization of ethylene initiated by PTFE radicals located on the surface. Molecular motion of peroxy radicals at the ends of IPE and NIPE chains tethered on the powder surface of PTFE was investigated in a vacuum in the temperature range from 3.4 to 223 K by ESR and a spectral simulation. The three kinds of motional mode of the ends of IPE chains were exhibited: (i) an isotropic tumbling motion of the ends on the PTFE surface with isotropic and slow rate in the temperature range from 30 to 113 K having E_{a1} 1.68 kJ/mol; (ii) an anisotropic tumbling motion of the ends on the PTFE surface with anisotropic rates in the range

120−213 K having E_{a2} 5.45 kJ/mol; (iii) a free rotational mode of the ends protruding from the PTFE surface with high and isotropic rate of 1.00×10^9 s^{-1}. The free-rotational mode is attributed to the noninteractions with both neighboring intra- and interchains of IPE. In contrast, the ends of NIPE chains exhibited the two kinds of motional mode: (i) an isotropic tumbling motion of the ends on the PTFE surface with isotropic and slow rate in the temperature range from 40 to 83 K having E_{a1} 1.87 kJ/mol; (ii) an anisotropic tumbling motion of the ends on the PTFE surface with anisotropic rates, in the temperature range from 93 to 223 K, having E_{a2} 2.77 kJ/mol. Even at 223 K, the tumbling motion of the ends still had anisotropic rates of 1.18×10^8 and 6.25×10^8 s^{-1}. The slow and anisotropic rates of the ends of NIPE chains on the PTFE surface are attributed to the interactions with both neighboring intra- and interchains of NIPE.

Any isolated polymer chain, which is freed from the interaction with surrounding matrix, should have high mobility even below the grass transition temperature in the bulk.

References and Notes

(1) Matsuoka, S.; Quan, X. *Macromolecules* **1991**, *24*, 2770.
(2) Mano, J. F. *Macromolecules* **2001**, *34*, 8825.
(3) Doruker, P.; Mattice, W. L. *Macromolecules* **1999**, *32*, 194.
(4) Jang, J. H.; Mattice, W. L. *Macromolecules* **2000**, *33*, 1467.
(5) Jang, J. H.; Ozisik, R.; Mattice, W. L. *Macromolecules* **2000**, *33*, 7663.
(6) Kajiyama, T.; Tanaka, K.; Takahara, A. *Macromolecules* **1997**, *30*, 280.
(7) Satomi, N.; Takahara, A.; Kajiyama, T. *Macromolecules* **1999**, *32*, 4474.
(8) Kawaguchi, D.; Tanaka, K.; Takahara, A.; Kajiyama, T. *Macromolecules* **2001**, *34*, 6164.
(9) Sakaguchi, M.; Yamaguchi, T.; Shimada, S.; Hori, Y. *Macromolecules* **1993**, *26*, 2612.
(10) Sakaguchi, M.; Shimada, S.; Hori, Y.; Suzuki, A.; Kawaizumi, F.; Sakai, M.; Bandow, S. *Macromolecules* **1995**, *28*, 8450.
(11) Sakaguchi, M.; Shimada, S.; Yamamoto, K.; Sakai, M. *Macromolecules* **1997**, *30*, 3620.
(12) Sakaguchi, M.; Shimada, S.; Yamamoto, K.; Sakai, M. *Macromolecules* **1997**, *30*, 8521.
(13) Yamamoto, K.; Shimada, S.; Tsujita, Y.; Sakaguchi, M. *Polymer* **1997**, *38*, 6327.
(14) Sakaguchi, M.; Yamamoto, K.; Shimada, S.; Sakai, M. *J. Polym. Sci., Part B: Polym. Phys.* **1998**, *36*, 2095.
(15) Yamamoto, K.; Suenaga, S.; Shimada, S.; Sakaguchi, M. *Polymer* **2000**, *41*, 6573.
(16) *CRC Hand Book of Chemistry and Physics*, 76th ed.; Lide, D. R., Ed.; CRC Press: Boca Raton, FL, 1995−1996; p 13-4.
(17) Shimada, S.; Suzuki, A.; Sakaguchi, M.; Hori, Y. *Macromolecules* **1996**, *29*, 973.
(18) Yamamoto, K.; Shimada, S.; Ohira, K.; Sakaguchi, M.; Tsujita, Y. *Macromolecules* **1997**, *30*, 6575.
(19) Sakaguchi, M.; Yamamoto, K.; Shimada, S. *Macromolecules* **1998**, *31*, 7829.
(20) Sakaguchi, M.; Sohma, J. *J. Polym. Sci., Polym. Phys. Ed.* **1975**, *13*, 1233.
(21) Binsch, G. *Mol. Phys.* **1968**, *15*, 469.
(22) Binsch, G. *J. Am. Chem. Soc.* **1969**, *91*, 1304.
(23) Heinzer, J. *Mol. Phys.* **1971**, *22*, 167.
(24) Sakaguchi, M.; Sohma, J. *J. Appl. Polym. Sci.* **1978**, *22*, 2915.
(25) Yamamoto, K.; Shimada, S.; Sakaguchi, M.; Tsujita, Y. *Polym. J.* **1997**, *29*, 370.
(26) Yamamoto, K.; Shimada, S.; Sakaguchi, M.; Tsujita, Y.; Sakaguchi, M. *Macromolecules* **1997**, *30*, 1776.
(27) *CRC Hand Book of Chemistry and Physics*, 76th ed.; Lide, D. R., Ed.; CRC Press: Boca Raton, FL, 1995−1996; p 6-57.
(28) *CRC Hand Book of Chemistry and Physics*, 76th ed.; Lide. D. R., Ed.; CRC Press: Boca Raton, FL, 1995−1996; p 9-31.
(29) Flory, P. J. *Statistical Mechanics of Chain Macromolecules;* John Wiley & Sons: New York, 1969.
(30) Mattice, W. L.; Helfer, C. A.; Sokolov, A. P. *Macromolecules* **2003**, *36*, 9924.
(31) Suryanarayana, D.; Kevan, L.; Schlick, S. *J. Am. Chem. Soc.* **1982**, *104*, 668.
(32) Padding, J. T.; Briels, W. J. *J. Chem. Phys.* **2001**, *115*, 2846.

MA049194J